

Supplementary information

for

Nanoencapsulation strategy: Enabling electrochemiluminescence of thermally activated delayed fluorescence (TADF) emitters in aqueous media

Zihui Zeng ^a, Ping Huang ^a, Yi Kong ^a, Lianpeng Tong ^a, Baohua Zhang ^{a*}, Yelin Luo ^a, Lijuan Chen ^a, Yuwei Zhang ^a, Dongxue Han ^a and Li Niu ^{a*}

^a Centre for Advanced Analytical Science, c/o School of Chemistry and Chemical Engineering, Guangzhou University, Guangzhou 510006, P. R. China.

*Corresponding authors.

E-mail address: ccbhzhang@gzhu.edu.cn (B.-H. Zhang), lniu@gzhu.edu.cn (L. Niu).

Materials

The TADF emitter, i.e. 1,2,3,5-tetrakis(carbazol-9-yl)-4,6-dicyanobenzene (4CzIPN) was purchased from Xi'an Polymer Light Technology Corp. The amphiphilic polymer, i. e. 1,2-distearoyl-sn-glycero-3-phosphoethanolamine-N-[methoxy(polyethylene glycol) 2000] (DSPE-PEG2000) was provided by Shanghai Ponsure Biotech, Inc. Tetrahydrofuran (THF, $\geq 99.9\%$) was obtained from Sigma-Aldrich Co. Ltd. (Shanghai, China). Tripropylamine (TPrA, $\geq 98\%$) and tetra-n-butylammonium hexafluorophosphate (TBAPF₆, 98%) were purchased from Alfa Co. Ltd. Potassium nitrate (KNO₃), potassium hydrogen phosphate (K₂HPO₄) and dipotassium phosphate (KH₂PO₄) were purchased from Sinopharm Chemical Reagent Co. Ltd (Shanghai, China). Ultrapure water was obtained from a Millipore water purification system ($>18.2\text{ k}\Omega$ Milli-Q, Millipore). All these reagents and chemicals were commercially available and used without further purification. All the aqueous CV and ECL measurement used phosphate buffered solution (PBS, pH = 7.43) containing 0.1 M KNO₃, 0.1 M K₂HPO₄ and 0.1 M KH₂PO₄ as the electrolyte.

Characterization method

Dynamic light scattering (DLS) experiment was conducted by using Nano-ZS equipment (Malvern Instruments, U.K.). Transmission electron microscope (TEM) images were obtained by using the JEM-2100F (JEOL, Japan) at an acceleration voltage of 200 kV. UV-vis absorption was acquired by the UV-1780 UV-VIS spectrophotometer (Shimadzu Co.). Edinburgh fluorescence spectrometer (FLS1000) was used for photophysical measurement, in which steady-state PL, time-gated PL and transient PL measurements were triggered by Xe₂ xenon lamp, microsecond lamp and a picosecond pulsed LED (EPLD-365), respectively, and a built-in integration sphere accessory was used to measure absolute PL quantum yield (PLQY) in air. The corresponding photophysical parameter shown in Table S1-S2 was obtained by the routine TADF photophysics theory.^{S1, S2} Redox electrochemistry experiments were conducted on a CHI 660B electrochemistry workstation (CH Instruments Inc.). ECL

measurements were carried out on a Xi'an Remex MPI-EII ECL system.

Preparation of the 4CzIPN nanoparticle (NPs) solutions

The 4CzIPN NPs in aqueous solution was prepared by a modified nanoprecipitation method.^{S3} For the typical preparation procedures, a mixture of 0.5 mg 4CzIPN and 1.0 mg DSPE-PEG2000 were dissolved in 2 mL THF. Then, the solution was sonicated for 20 min. to obtain a homogeneous clarified solution. After that, the solution was rapidly added to 10 mL of ultrapure water in a bath sonicator, followed by uninterrupted ultrasound treatment for 3 min. After that, the THF solvent was removed and the solution was concentrated to 2 mL through rotary evaporation under vacuum. Finally, the 4CzIPN NPs solution was filtered through poly(ether sulfone) (PES) syringe filter (the intercept aperture: 0.22 μm) to filter out the possible large aggregates. The resulting 4CzIPN aqueous nanodispersion was transparent and yellow in color by observation under naked eyes, and emitted bright yellow in color under the UV excitation at 365 nm. It was stable and could be stored at 4 °C for several months without noticeable aggregation.

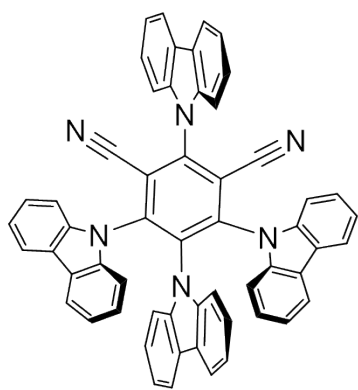
CV Measurement

The CV experiments were tested on a CHI 660B electrochemistry workstation (CH Instruments Inc.). Generally, a three-electrode system (a Pt wire as a counter electrode, a Ag wire or Ag/AgCl as a reference electrode, a glassy carbon electrode (GCE) with a diameter of 4 mm as a working electrode) was used, which was calibrated by using ferrocene (Fc)/ferrocenium (Fc⁺) couple. CVs of 4CzIPN was tested in acetonitrile (MeCN) with 0.1 M TBAPF₆ as supporting electrolyte under nitrogen atmosphere and scan rate of 100 mV s⁻¹.

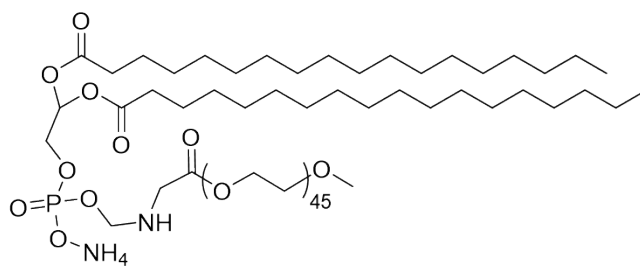
ECL Measurement

Electrochemiluminescence (ECL) was conducted on a MPI-EII ECL (Remex Electronic Instrument Lt. Co., Xi'an, China) detection system. For aqueous ECL

measurement experiments, a three-electrode system (a Pt wire as a counter electrode, Ag/AgCl (saturation KCl solution) as a reference electrode, a glassy carbon electrode (GCE) with a diameter of 4 mm as a working electrode) was used, with a photomultiplier tube (PMT) voltage of 850 V. The three-electrode system was immersed in PBS solution (pH = 7.43) containing 4CzIPN NPs (25 $\mu\text{g mL}^{-1}$ in concentration) for the ECL tests, and the whole system was tested in ambient conditions. Co-reactant ECL studies were conducted using the same procedures except for additionally adding 30 mM TPrA into such solution. The ECL efficiency of 1 $\mu\text{M Ru}(\text{bpy})_3^{2+}$ containing 30 mM TPrA in the same tested medium was taken the standard reference for calculating the relative ECL efficiency (Φ_{ECL}).^{S4} As measured and calculated using routine method,^{S5} the Φ_{ECL} of 4CzIPN NPs/TPrA couple relative to the $\text{Ru}(\text{bpy})_3^{2+}/\text{TPrA}$ system was calculated to be 0.7 %.



4CzIPN



DSPE-PEG2000

Figure S1. Chemical Structures of 4CzIPN and DSPE-PEG2000.

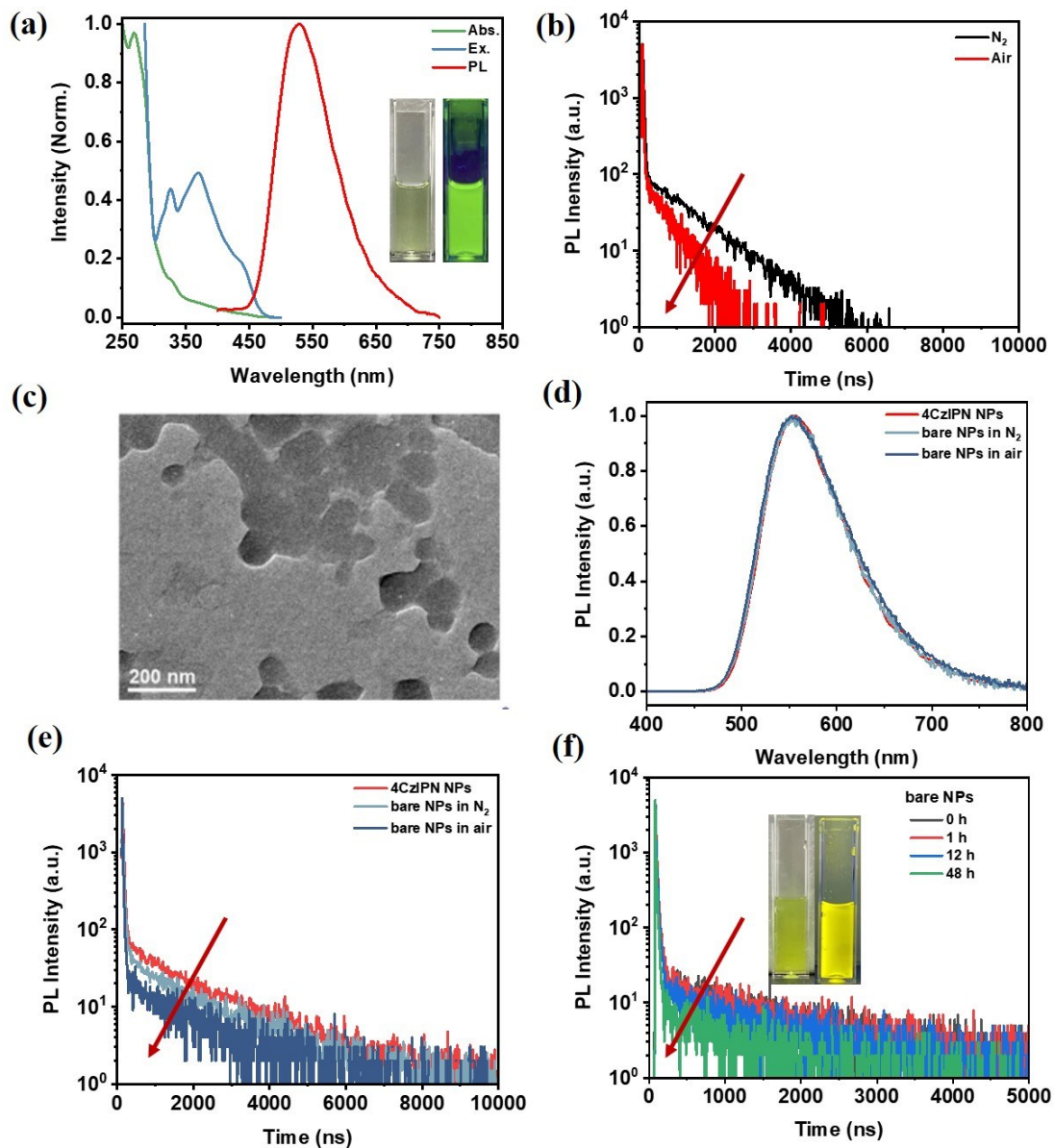


Figure S2. (a) UV-vis absorption, PL excitation, PL spectra of 4CzIPN in THF (1×10^{-5} M). Inset: 4CzIPN under daylight (left) and 365 nm excitation (right). $\lambda_{\text{EX}} = 365$ nm. (b) Transient PL decay curves of 4CzIPN in THF in N_2 or in air. (c) TEM image of 4CzIPN bare NPs (i.e. without shielding polymer DSPE-PGE2000). (d) Steady-state PL spectra of NPs and bare NPs in N_2 or in air. (e) Comparison of PL transient decay curves of NPs and bare NPs in different conditions. (f) Comparison of PL transient decay curves of bare NPs under different storage time (inserted picture: 4CzIPN bare NPs dispersions under daylight (left) and 365 nm excitation (right)).

Table S1. Photophysical properties of 4CzIPN in THF solvent or in aqueous solution (NPs).

Form	λ_{PL} [nm]	Fwhm [nm]	τ_{p} [ns]	τ_{d} [ns]	A_1	A_2	Φ_{PL} [%]	χ^2
THF solution ^a	527	104	22.9	1184	359	4.34	n. a.	1.297
THF solution ^b	527	105	18.0	549	5878	91.2	16.76	1.211
NP solution ^a	555	99	22.1	1879	15583	213	n. a.	1.103
NP solution ^b	555	101	21.9	1797	15889	170	21.56	1.110

^a measured under N₂ protection; ^b measured in air. For the τ_{p} and τ_{d} , they are the exciton lifetime of prompt fluorescent component and delayed fluorescent component of 4CzIPN, respectively, which is calculated by standard exponential fitting methods on the PL decay curves as measured.^{S6}

Notation:

Obviously, as depicted in Figure S2 and Table S1, delayed fluorescent component of 4CzIPN in THF solution is seriously lowered, along with sharply reduced delayed fluorescent lifetime, i.e. τ_{d} , from 1184 ns to 549 ns, which is due to oxygen quenching effect on the triplets of 4CzIPN.^{S7} By contrast, transient PL decay characteristics of 4CzIPN NPs are barely influenced by environment atmosphere and even storage in air (see Figure 1d) and Table S1. Considering the sensitive oxygen-quenching effect of TADF emitters, such results will confirm that nanoencapsulation strategy using the amphiphilic polymer DSPE-PEG2000 is success, which well protect the core component, i.e. 4CzIPN, from oxygen quenching in air. Also, it was found that for the control sample, i.e. bare TADF-NPs without using capping polymer DSPE-PEG2000, its NPs tend to aggregate in morphology, and their photophysical properties are very unstable and sensitive to oxygen and air condition (gradually quenched as increasing the exposure time). Moreover, the PL quantum efficiency of the as-prepared bared NPs is significantly lowered to 10.48% (vs. 21.56% for the NPs using encapsulation strategy, see Table S2). Accordingly, it was confirmed that encapsulation strategy on

TADF-NPs with shielding polymer, e.g. DPSE-PEG2000 shown here, is indispensable for achieving such air-stable TADF-type NPs in aqueous media.

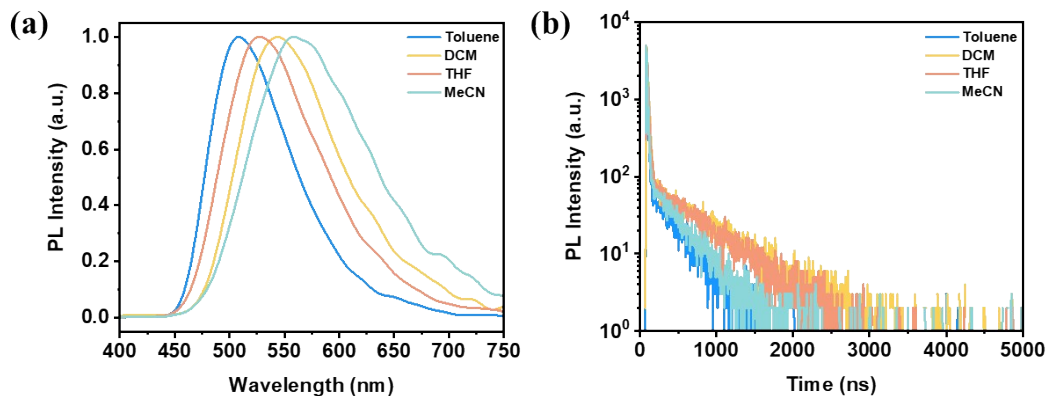


Figure S3. (a) PL spectra and (b) transient PL decay curves of 4CzIPN in different solvent (1×10^{-5} mol L⁻¹), including toluene, DCM, THF and MeCN, measured in atmosphere (excitation condition: $\lambda_{\text{Ex}} = 365$ nm).

Table S2. Summary of the photophysical properties of 4CzIPN dissolved in different solvent and 4CzIPN NPs and bare NPs (i.e. without capping polymer DSPE-PGE2000).

Conditions	λ_{PL}^a [nm]	Fwhm [nm]	Φ_{PL}^b [%]	τ_p^c [ns]	τ_d^c [ns]	Φ_{PF}^d [%]	Φ_{DF}^d [%]	k_f^e [10 ⁶ s ⁻¹]	k_{ISC}^f [10 ⁷ s ⁻¹]	k_{RISC}^g [10 ⁵ s ⁻¹]
Toluene	508	87	16.29	11.5	315	12.26	4.03	10.6	9.91	84.7
DCM	544	105	19.94	19.8	647	13.77	6.17	6.95	5.86	29.7
THF	527	104	16.76	18	549	11.39	5.37	6.33	6.27	34.2
MeCN	566	126	7.40	12.8	334	5.21	2.19	4.07	8.24	67.5
NPs	555	101	21.56	21.9	1797	10.82	10.74	4.94	5.12	5.00
bare NPs	555	103	10.48	18.9	1157	7.50	2.98	3.97	5.72	20.1

^a Measured at room temperature in air. ^b Absolute PLQY evaluated using an integrating sphere under air atmosphere. ^c The prompt fluorescence lifetime (τ_p) and the delayed fluorescence lifetime (τ_d) calculated by transient PL decay curves under air atmosphere at room temperature, the average lifetime calculated by $\tau_{\text{av}} = \sum A_i \tau_i^2 / \sum A_i \tau_i$, where A_i is the pre-exponential for lifetime τ_i . ^d The fractional contributions of the prompt fluorescence (Φ_{PF}) and delayed fluorescence (Φ_{DF}) to the total Φ_{PL} calculated by transient PL decay curves under air atmosphere. $\Phi_{\text{PL}} = \Phi_{\text{PF}} + \Phi_{\text{DF}}$, $\Phi_{\text{PF}} = r_p \times \Phi_{\text{PL}}$, $r_p = \tau_1 A_1 / (\tau_1 A_1 + \tau_2 A_2 + \tau_3 A_3)$, $\Phi_{\text{DF}} = r_d \times \Phi_{\text{PL}}$, $r_d = 1 - r_p$. ^e The fluorescence rate constants of S_1 calculated using equation of $k_f = \Phi_{\text{PF}} / \tau_p$. ^f The rate constants of ISC calculated

using equation of $k_{ISC} = 1/\tau_p(1-\Phi_{PF})$. ^s The rate constant of RISC rate was calculated using equation of $k_{RISC} = (k_p k_d)/k_{ISC} \times (\Phi_{DF}/\Phi_{PF})$, in which $k_p = 1/\tau_p$, $k_d = 1/\tau_d$.

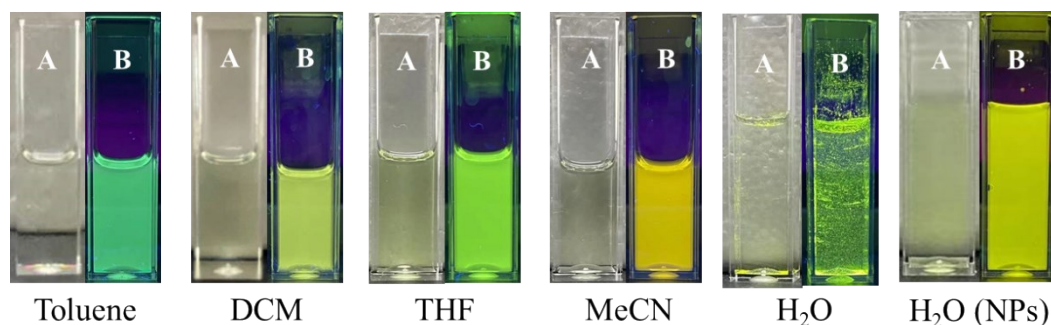


Figure S4. Photograph of 4CzIPN in different solvent (10^{-5} M) and NPs dispersion under daylight (A) and 365 nm excitation (B).

Notation:

Due to extremely low solubility of 4CzIPN in water, the corresponding solution is inhomogeneous. A lot of 4CzIPN powder sticks to the walls of the quartz pool. By contrast, 4CzIPN NPs are homogenous and stable in water.

Table S3. Summary of PL property of 4CzIPN in different solvent and NPs dispersions.

Solvent	Toluene	DCM	THF	MeCN	H ₂ O (NPs)
polarity	2.4	3.4	4.2	6.2	10.2
λ_{PL}^a [nm]	508	544	527	566	555

^a Measured in air atmosphere.

Notation:

Basically, except for DCM, with increasing the polarity of solvent, the PL emission of 4CzIPN is monotonically redshifted, which is due to the stabilization effect of polar solvent for such TADF emitters with strong charge transfer (CT) state in nature. ^{s8}

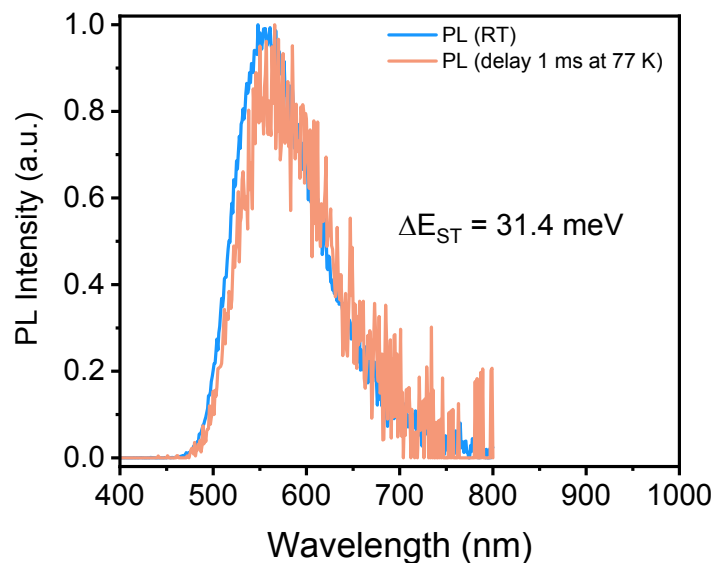


Figure S5. Photoluminescence and phosphorescence spectra of 4CzIPN NPs ($25 \mu\text{g mL}^{-1}$ in concentration) under air atmosphere. $\lambda_{\text{Ex}} = 365 \text{ nm}$.

Table S5. Electrochemical data of 4CzIPN and the calculated energy levels and energy gap.

Molecule	$E_{\text{onset}}^{\text{Ox}}$ [V]	$E_{\text{onset}}^{\text{Red}}$ [V]	$E_{\text{HOMO}}^{\text{b}}$ [eV]	$E_{\text{LUMO}}^{\text{b}}$ [eV]	$E_{\text{gap}}^{\text{b}}$ [eV]
4CzIPN	1.41	-1.15	-5.87	-3.1	2.77

^a Potential was versus Ag/Ag^+ . ^b Fc/Fc^+ couple was used as the internal reference. The energy levels were calculated using the following equations:

$$E_{\text{HOMO}} = -\left(E_{\text{onset}}^{\text{Ox}} - E_{\text{Fc}/\text{Fc}^+} + 4.8\right) \text{ eV},$$

$$E_{\text{LUMO}} = -\left(E_{\text{onset}}^{\text{Red}} - E_{\text{Fc}/\text{Fc}^+} + 4.8\right) \text{ eV}, E_{\text{gap}} = E_{\text{LUMO}} - E_{\text{HOMO}}.$$

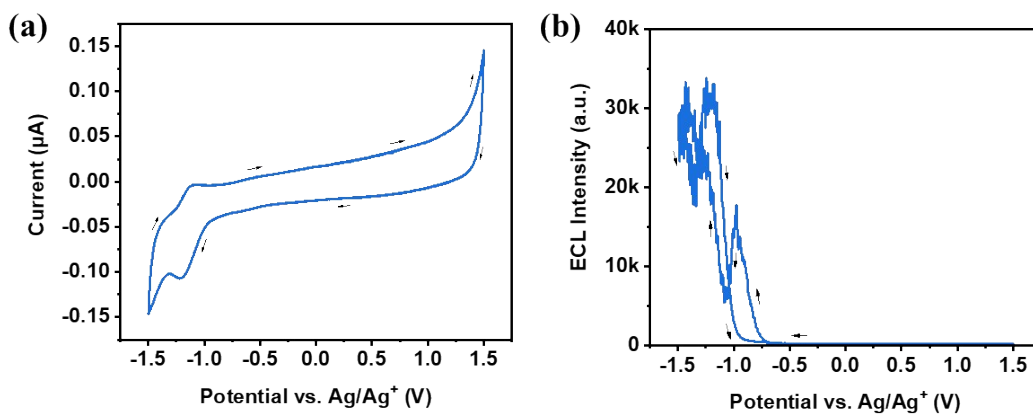


Figure S6. (a) Cyclic voltammograms and (b) the corresponding annihilation ECL of 0.1 mM 4CzIPN measured in the nitrogen-saturated MeCN solution containing 0.1 M TBAPF₆. Scan rate: 100 mV s⁻¹.

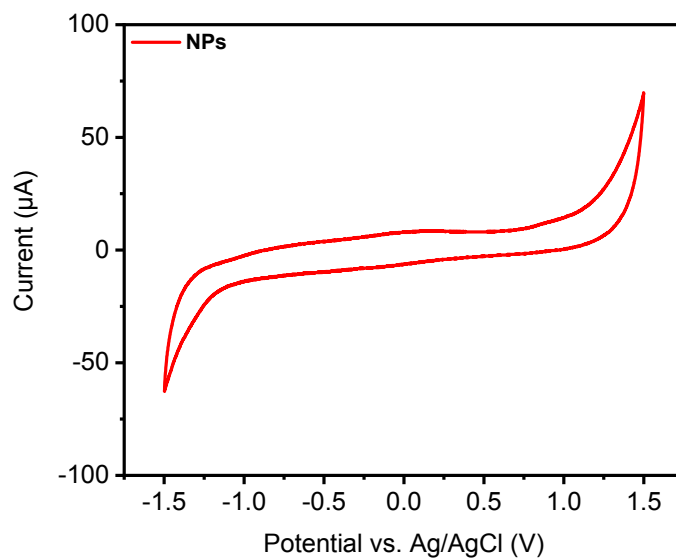


Figure S7. Cyclic voltammograms of 4CzIPN NPs in the PBS solution (0.1 M, pH = 7.43). Scan rate: 100 mV s⁻¹.

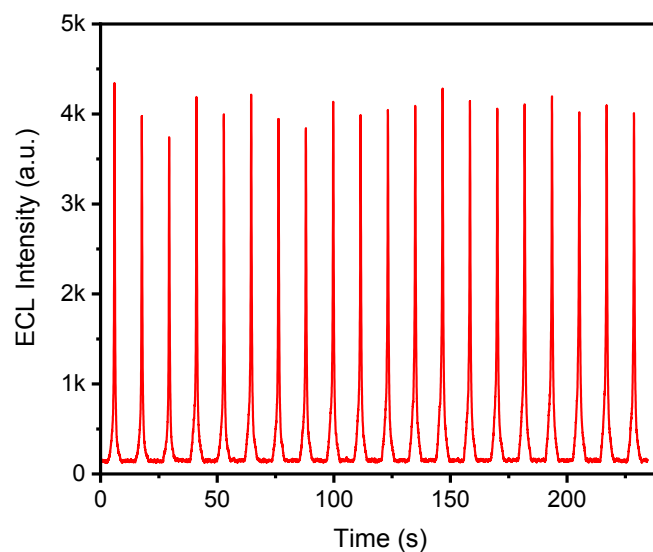


Figure S8. Oxidative-reduction ECL stability of 4CzIPN NPs with 30 mM TPrA in PBS solution (0.1 M, pH = 7.43). Scan rate: 100 mV s⁻¹.

Reference:

- S1. Y. Tao, K. Yuan, T. Chen, P. Xu, H. Li, R. Chen, C. Zheng, L. Zhang and W. Huang, *Adv. Mater.*, 2014, **26**, 7931-7958.
- S2. X. Lin, Y. Zhu, B. Zhang, X. Zhao, B. Yao, Y. Cheng, Z. Li, Y. Qu and Z. Xie, *ACS Appl. Mater. Interfaces*, 2018, **10**, 47-52.
- S3. Y. Feng, C. Dai, J. Lei, H. Ju and Y. Cheng, *Anal. Chem.*, 2016, **88**, 845-850.
- S4. S. Feng, Z. Wang, Y. Feng, Y. Cheng, H. Ju, Y. Quan, *Biosensors Bioelectron.* 2018, **100**, 28-34.
- S5. F. Wang, J. Lin, T. Zhao, D. Hu, T. Hu, Y. Liu, *J. Am. Chem. Soc.* 2016, **138**, 7718-7724.
- S6. T. Nakagawa, S.-Y. Ku, K.-T. Wong and C. Adachi, *Chem. Commun.*, 2012, **48**, 9580-9582.
- S7. R. Ishimatsu, Y. Kirino, C. Adachi, K. Nakano and T. Imato, *Chem Lett*, 2016, **45**, 1183-1185.
- S8. R. Ishimatsu, S. Matsunami, K. Shizu, C. Adachi, K. Nakano and T. Imato, *J. Phys. Chem. A*, 2013, **117**, 5607-5612.